

AD-A128 677

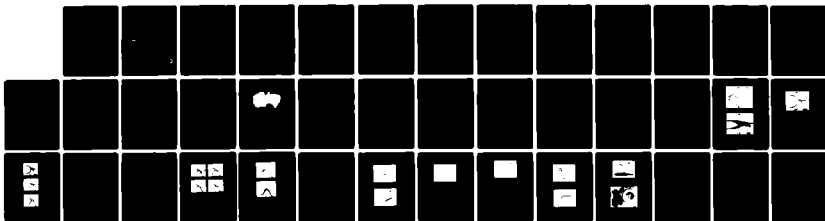
ORIENTATION INDEPENDENT IGNITRON(U) HUGHES AIRCRAFT CO
MALIBU CALIF R J HARVEY ET AL. FEB 83 AFWL-TR-82-115
F29601-80-C-0058

1/1

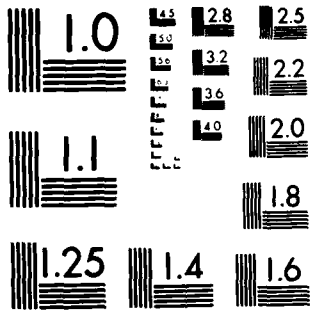
UNCLASSIFIED

F/G 9/1

NL



END
DATE
FILMED
6-83
DTIC



MICROCOPY RESOLUTION TEST CHART
NATIONAL BUREAU OF STANDARDS-1963-A

2

AD A 128677

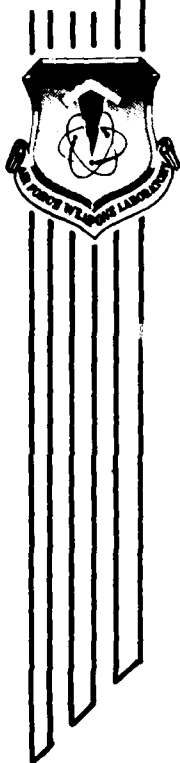
ORIENTATION INDEPENDENT IGNITRON

R. J. Harvey
H. E. Gallagher

Hughes Aircraft Company
3011 Malibu Canyon Road
Malibu, CA 90265

February 1983

Final Report



Approved for public release; distribution unlimited.

DTIC FILE COPY

AIR FORCE WEAPONS LABORATORY
Air Force Systems Command
Kirtland Air Force Base, NM 87117

DTIC
ELECTE
MAY 27 1983
S E D

83 05 20 020

This final report was prepared by the Hughes Aircraft Company, Malibu, California, under Contract F29601-80-C-0058, Job Order 317J0526 with the Air Force Weapons Laboratory, Kirtland Air Force Base, New Mexico. Mr. James P. O'Loughlin (ARAY) was the Laboratory Project Officer-in-Charge.

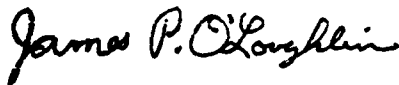
When Government drawings, specifications, or other data are used for any purpose other than in connection with a definitely Government-related procurement, the United States Government incurs no responsibility or any obligation whatsoever. The fact that the Government may have formulated or in any way supplied the said drawings, specifications, or other data, is not to be regarded by implication, or otherwise in any manner construed, as licensing the holder, or any other person or corporation; or as conveying any rights or permission to manufacture, use, or sell any patented invention that may in any way be related thereto.

This report has been authored by a contractor of the United States Government. Accordingly, the United States Government retains a nonexclusive, royalty-free license to publish or reproduce the material contained herein, or allow others to do so, for the United States Government purposes.

This report has been reviewed by the Public Affairs Office and is releasable to the National Technical Information Service (NTIS). At NTIS, it will be available to the general public, including foreign nations.

If your address has changed, if you wish to be removed from our mailing list, or if your organization no longer employs the addressee, please notify AFWL/ARAY, Kirtland AFB, NM 87117 to help us maintain a current mailing list.

This technical report has been reviewed and is approved for publication.



JAMES P. O'LOUGHLIN
Project Officer



THOMAS W. MEYER
Lt Colonel, USAF
Chief, Advanced Laser Branch

FOR THE COMMANDER



DAVID W. SEEGMILLER
Colonel, USAF
Chief, Advanced Laser Tech Division

DO NOT RETURN COPIES OF THIS REPORT UNLESS CONTRACTUAL OBLIGATIONS OR NOTICE ON A SPECIFIC DOCUMENT REQUIRES THAT IT BE RETURNED.

UNCLASSIFIED

SECURITY CLASSIFICATION OF THIS PAGE (When Data Entered)

REPORT DOCUMENTATION PAGE		READ INSTRUCTIONS BEFORE COMPLETING FORM
1. REPORT NUMBER AFWL-TR-82-115	2. GOVT ACCESSION NO. AD-A128677	3. RECIPIENT'S CATALOG NUMBER
4. TITLE (and Subtitle) ORIENTATION INDEPENDENT IGNITRON		5. TYPE OF REPORT & PERIOD COVERED Final Report
		6. PERFORMING ORG. REPORT NUMBER
7. AUTHOR(s) R. J. Harvey H. E. Gallagher		8. CONTRACT OR GRANT NUMBER(s) F29601-80-C-0058
9. PERFORMING ORGANIZATION NAME AND ADDRESS Hughes Aircraft Company 3011 Malibu Canyon Road Malibu, CA 90265		10. PROGRAM ELEMENT, PROJECT, TASK AREA & WORK UNIT NUMBERS 63605F/317J0526
11. CONTROLLING OFFICE NAME AND ADDRESS Air Force Weapons Laboratory (ARAY) Kirtland Air Force Base, NM 87117		12. REPORT DATE February 1983
		13. NUMBER OF PAGES 38
14. MONITORING AGENCY NAME & ADDRESS (if different from Controlling Office)		15. SECURITY CLASS. (of this report) Unclassified
		15a. DECLASSIFICATION/DOWNGRADING SCHEDULE
16. DISTRIBUTION STATEMENT (of this Report) Approved for public release; distribution unlimited.		
17. DISTRIBUTION STATEMENT (of the abstract entered in Block 20, if different from Report)		
18. SUPPLEMENTARY NOTES		
19. KEY WORDS (Continue on reverse side if necessary and identify by block number) Ignitron Repetitive Switch Trigger Stability Jitter		
20. ABSTRACT (Continue on reverse side if necessary and identify by block number) The orientation independent ignitron is a closing switch suitable for high average power and mobile applications. This report describes work performed to reduce the switch jitter and improve stability. Improvements are described which reduce switch rms-jitter times from 300 ns to less than 20 ns and enable run times to exceed 180 s at 100 p/s and 6-kW average power. These improvements include stabilizing the ignitor temperature by reducing the trigger energy from 2 J to 30 mJ. Stabilization of the background mercury pressure is also shown (Over)		

DD FORM 1 JAN 73 1473

UNCLASSIFIED
SECURITY CLASSIFICATION OF THIS PAGE (When Data Entered)

UNCLASSIFIED

SECURITY CLASSIFICATION OF THIS PAGE(When Data Entered)

10. ABSTRACT (Continued)

to lead to stabilization of the anode current pulse shape. Additional switch instabilities have been identified at higher average power. These instabilities are: (1) failure to trigger properly because contamination blocks mercury migration on the cathode surface, and (2) over-pressure breakdown caused by the evolution of contaminate gases or overheating of the cathode. A switch design is described which takes these factors into account and is estimated to have a 90-s stable run time with 30-kV, 15-kA, and 10- μ s pulses at 100 p/s.

UNCLASSIFIED

SECURITY CLASSIFICATION OF THIS PAGE(When Data Entered)

PREFACE

This project was monitored by Mr. James O'Loughlin at AFWL/KAFB and managed by Dr. Robin J. Harvey at Hughes Research Laboratories.

The authors wish to express their appreciation to Messrs. A.R. Kramer and R.G. Fleig for their testing and construction assistance, and to Dr. A.J. Palmer for statistical computer analysis. We are also indebted to Mr. James O'Loughlin for his assistance in the use of the test facilities at Kirtland Air Force Base.

Accession For		
NTIS GRA&I	<input checked="" type="checkbox"/>	
DTIC TAB	<input type="checkbox"/>	
Unannounced	<input type="checkbox"/>	
Justification		
By _____		
Distribution/ _____		
Availability Codes		
_____ and/or		
Dist	Special	
A		



CONTENTS

SECTION		PAGE
I.	INTRODUCTION AND SUMMARY	7
II.	TRIGGER STABILITY	12
	1. Experimental Apparatus	13
	2. Low Power Test Results Using a Conventional Ignitor System	16
	3. Jitter Time Correlation Between Pulses	18
	4. Test Results with a Modified Ignitor System.....	18
	5. Repetition Rate Effects (Trigger)	20
	6. Anode Conduction Behavior	20
	7. Multiple Ignitors	24
	8. Repetition Rate Effects with Anode Current	27
	9. Summary of Trigger Improvements	27
III.	HIGH AVERAGE POWER TESTS	30
	1. High Power Test Results Using OII-3	30
	2. High Power Tests of OII-2	33
	3. Analysis of the Cathode Surface	33
	4. Discussion of Results	36
	5. Summary of High Average Power Test Results	37
IV.	DESIGN CONSIDERATIONS FOR A HIGH AVERAGE POWER OII	38

ILLUSTRATIONS

FIGURES		PAGE
1	Cross-Sectional View of OII-2	8
2	High average power OII design	11
3	Cross-sectional view of OII-3	14
4	OII-3 completed assembly showing mercury-fill and pump-out plumbing	15
5	Test circuit for OIIs	15
6	Pulsed ignitor characteristics	17
7	Interpulse correlation coefficient for jitter time for 124 observations using sample data taken at 1 and and 2 Hz, using a conventional ignitor system	19
8	Characteristic conditions for external avalanche breakdown along the ignitor	21
9	Ignitor arc delay time	22
10	Operation at peak anode current of 18 kA	23
11	Operation at 100 Hz	23
12	Anode voltage fall and current rise	24
13	Jitter as a function of the number of ignitors in use	25
14	Low-repetition-rate jitter (σ) and delay (Δt) times as a function of ignitor capacitor voltage	26
15	Jitter as a function of Pulse repetition rate	28
16	Jitter as a function of OII Hg pressure	29
17	Anode current pulse, 1 kA \times 28 μ s, 400 A/D, 5 μ s/D	31
18	Anode current rise showing jitter at 100 Hz for a 90 s run period, 400 A/D, 200 ns/ Δ , $\sigma \cong$ 30 ns	31
19	Anode recovery voltage at 5 kV/D, 1 ms/D	32

FIGURE		PAGE
20	Ignitor current pulse at 100 A/D, 200 ns/D showing residual trigger source generated jitter	33
21	Anode current pulse showing reverse conduction, 1 kA/D, 5 μ s/D	34
22	Anode recovery voltage for OII Mod 2, 5 kV/D, 1 ms/D	34
23	Anode current pulse showing missing pulses, 200 A/D, 5 μ s/D	35
24	Cathode for OII - 3, showing Hg depleted area (light region) and contaminated Hg layer (dark region)	35

I. INTRODUCTION AND SUMMARY

The orientation independent ignitron (OII) is an ignitron-type closing switch suitable for mobile applications (Ref. 1). It has the electrical characteristics of ignitrons, but with the added advantage of a mechanically stable cathode. This is accomplished by using a solid cathode covered by a mercury (Hg) film. The film is held in place by surface tension, making the device orientation and vibration insensitive. The mercury film is continuously replenished by migration and condensation which are enhanced by cooling the cathode. The anode of the OII is cooled by natural convection to the external environment during off-periods. OIIs have previously been operated at 30 kV, 15 kA, with 10- μ s-wide pulses at frequencies up to 100 Hz for short bursts. Reformation of the film occurred during and following the pulse burst with a thermal recycle time of about 10 min. The stability and jitter characteristics of the OII were identified as a limiting factor in the switch performance. The objective of this program was to reduce the jitter and extend the stable run time of the OII from 5 s to over 90 s at the high average power pulse conditions noted above.

At the start of the present work, it was assumed that mercury depletion in the neighborhood of the ignitor electrode (Fig. 1) was responsible for the erratic switching which occurred after several seconds of operation at high average power. Also evident was a crude correlation in time between the onset of this erratic switching behavior and the onset of fluctuations in the trigger current characteristics. Since proper switch operation cannot be achieved if the trigger is erratic, efforts were first concentrated on identifying and eliminating the trigger instability.

Section II describes the steps taken to reduce the switch rms-jitter time from 300 to less than 20 ns and to extend the stable run time of the switch to over 180 s at up to 6-kW average power. These steps include stabilizing the ignitor temperature by heat sinking the semiconducting ignitor tip and reducing the trigger-pulse energy from 2 J to 30 mJ. Start-up variations in the mercury pressure are also identified. These are due to cathode-temperature changes

1. R.J. Harvey and J.R. Bayless, "Orientation Independent Ignitron,"
Proceedings, 2nd IEEE International Pulsed Power Conference, Lubbock, Texas,
June 12-14, 1979.

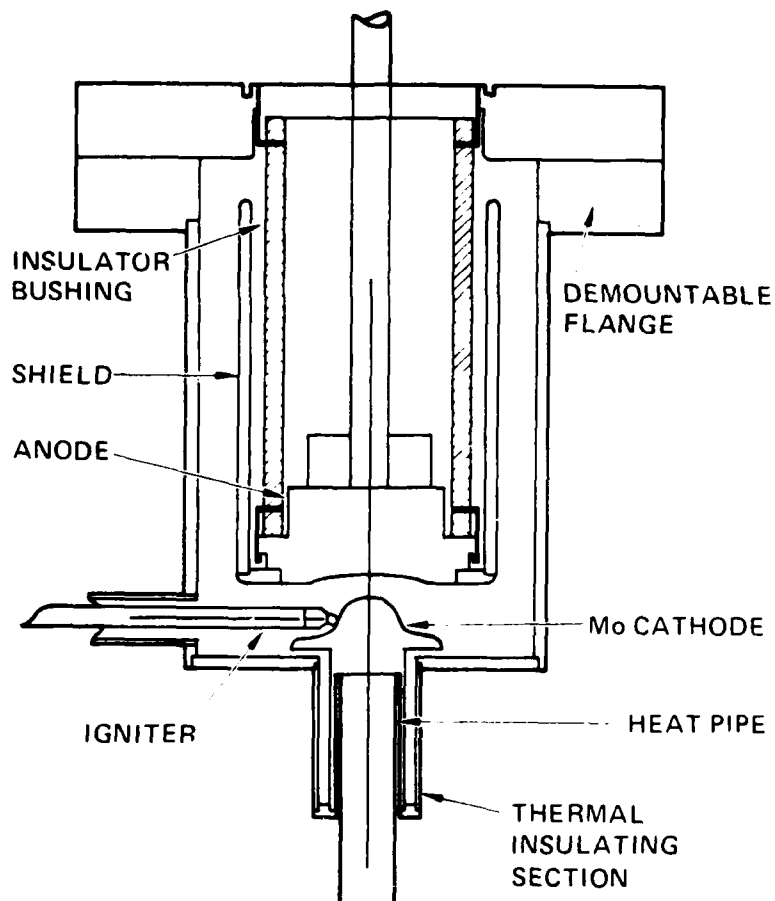


Figure 1. Cross-sectional view of OII-2.

which cause variations in the growth-rate of current (Table 1) and also contribute to jitter in the anode-current pulse before the switch reaches thermal equilibrium.

Section III describes the results of high-average power tests where additional sources of switch jitter and instability are identified, as shown in Table 1. These sources of instability include: (1) mercury starvation due to excessive heating of the cathode, (2) lack of migration of mercury due to contamination, and (3) over-pressurization due to contamination. The observed results of these instabilities are failure to trigger and failure to hold off voltage. The results of operation with multiple igniters show that a single

ignitor activates a region about 1 cm in radius. The need for multiple ignitors becomes important if mercury migration into the active region cannot be assured.

Section IV discusses the design of a high average power switch (Fig. 2) which takes these considerations into account. The switch design uses 1-kg molybdenum electrodes to increase the heat-sinking capability and to limit the flow of inverse current. A large cathode surface area is water cooled to provide additional heat rejection during operation. A sputter shield is extended partially over the ignitor and cathode electrodes to break the Paschen-breakdown path below the ignitors and partially protect the ignitors. The insulators are backed away from the arc region and are convoluted to further reduce the effects of sputtering. Multiple ignitors are included to extend the lifetime of the device. The overall weight of the tube design is less than 3 kg and it is less than 2000 cm³ in volume. Water or thermoelectric cooling of the anode is optional, depending on the usage. Trigger energy is less than 30 mJ per pulse. No keep-alive, heater or other auxiliary power is required.

TABLE 1. OPERATIONAL OII EFFECTS AND DESIGN CONSIDERATIONS

TRIGGER EFFECTS

<u>MECHANISM</u>	<u>EFFECT</u>	<u>CURE/RESULT</u>
Thermal instability in semi-conducting ignitor trigger	Trigger overheats Delay time increased RMS-Jitter > 300 ns Run time < 90 s	Lower trigger energy Heat sink trigger RMS-jitter < 20 ns Run time >> 180 s
Start up jitter due to pressure changes	Temperature of cathode increases causing mercury vapor pressure increase Delay time decreases then stabilizes	Establish thermal equilibrium as rapidly as possible Heat sink electrodes Preprogram delay of early pulses
Multiple Ignitors	Less power per ignitor/ more ignitors	No advantage
<u>HIGH POWER EFFECTS</u>		
Cathode heating	Increases mercury vapor Paschen breakdown Reduced recondensation rate of mercury Mercury starvation on cathode Jitter/failure to fire Accentuated by inverse current	Increase electrode heat capacity Increase cooling power Increase mercury volume Use molybdenum anode
Contamination	Outgassing Paschen breakdown Reacts with surface of mercury film Blocks migration of mercury Mercury starvation Jitter/failure to fire	High vacuum pre-processing Sealed-off units Use high purity components
Multiple Ignitors	Extend active region when surface partially mercury starved	Space 2 cm apart
Sputtering	Insulator coating Voltage hold-off failure Accentuated by inverse current/anode arc spot formation	Add sputter shield Convolute insulator Back insulator away Heat-sink anode Use molybdenum anode

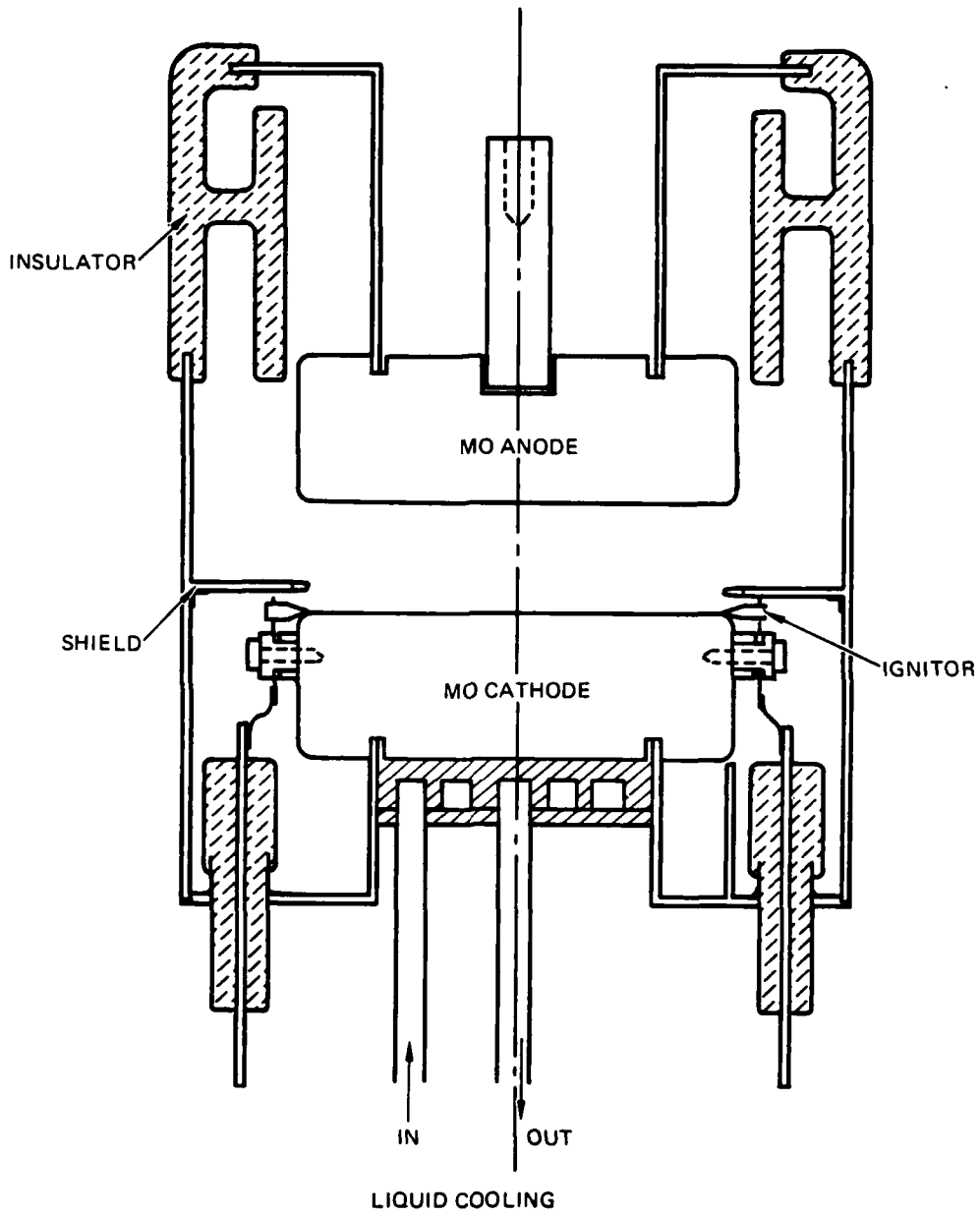


Figure 2. High average power OII design.

II. TRIGGER STABILITY

The OII has trigger characteristics comparable to conventional ignitrons. This section reports on advances in the design and operation of the ignitor electrode and in the trigger circuit which allow the OII to operate with jitter of less than 0.2 μ s at repetition rates in excess of 100 p/s and run periods of over 3 min. The jitter and trigger instability are related to (1) thermal variations in the semiconducting-ignitor resistance, (2) a rapidly varying voltage-time characteristic for trigger-arc development across the ignitor tip and (3) a pressure-voltage characteristic for the development of the main arc across the anode-to-cathode gap.

The passage of current through the conical ignitor to the mercury contact point has two effects. High electric fields are generated along the surface of the semiconductor, and both the semiconductor and mercury are ohmically heated. Both effects are strongest at the contact points; electrons and ionized mercury vapor are emitted from the contact point. This emission of plasma is limited and is not sufficient to produce anode conduction by itself. However, if the electric field exceeds a threshold value for a sufficiently long time, an avalanche develops along the ignitor tip to the supporting metallic structure and a cathode-arc spot forms, increasing the emission of plasma from the cathode. It is the formation of this ignitor arc that leads to the breakdown of the main anode-to-cathode gap. The anode-fall time is also an avalanche process and depends on the background pressure, which, in turn, is related to the cathode temperature.

If successive or excessive pre-arc ignitor currents heat the semiconducting tip, the resistance of the tip falls and the voltage drop across the ignitor may not be sufficient to initiate or sustain an arc. In this event, a relatively large amount of charge may pass through the ignitor without anode conduction taking place. By reducing the ignitor-power loading and improving the ignitor-heat rejection capability, it is possible to increase the repetition rate by orders of magnitude while reducing the switch jitter by an order of magnitude. While conventional practice would dictate a trigger energy of about 2 J, triggering is most reliable with trigger energies of about 30 mJ.

1. EXPERIMENTAL APPARATUS

The major components of the experimental apparatus consist of two models (denoted OII-2 and OII-3) of the Orientation Independent Ignitron (OII) and their test circuit. A cross-sectional view of OII-2 was shown in Figure 1. This is a single-ignitor OII. The cathode is made of molybdenum and is supported by thermally insulating stainless-steel cylinders. The cathode is cooled by a copper rod, attached to the cathode at one end, with the other end encased in a cooling coil. The ignitor is attached to an adjustable rod so that the ignitor tip-to-cathode spacing can be adjusted. The ignitor tip typically consists of molybdenum. The anode is supported on a ceramic bushing and shields are attached around the ceramic to both protect the ceramic from deposits of sputtered material and to prevent Paschen breakdown.

A cross-sectional view of the OII-3 is shown in Figure 3. This is a multiple-ignitor OII. Seven ignitors are positioned around the outer diameter of the cathode. Again the ignitor tips are carbide and the cathode is molybdenum. The ignitors are supported from the cathode assembly. This provides a means of keeping the ignitor tips in contact with the cathode at the required pressure and also cools the ignitors by thermal conduction to the chilled cathode. This cathode is also cooled with a copper rod attached to a cooling coil. The shields around the ignitors and the anode cylinder provide some protection against both sputtered material and Paschen breakdown. Both of these experimental models of the OII were fabricated using demounted flanges. Figure 4 is a photograph of the OII-3, which also shows the mercury-fill and pump-out plumbing.

The basic test circuit and typical component values are shown in Figure 5. The rise time of the ignitor current is determined by both the No. 6279 hydrogen thyatron and inductance of the loop through the thyatron, capacitors and ignitors. The approximate inductance of this loop is $3\mu\text{H}$. The inductance of the anode loop is about $0.5\mu\text{H}$, which determines, in part, the rise time of the anode current. The anode capacitor was increased from 0.1 to $4\mu\text{F}$ to lower the loop impedance for high current (15 kA) measurements. The dc current limit

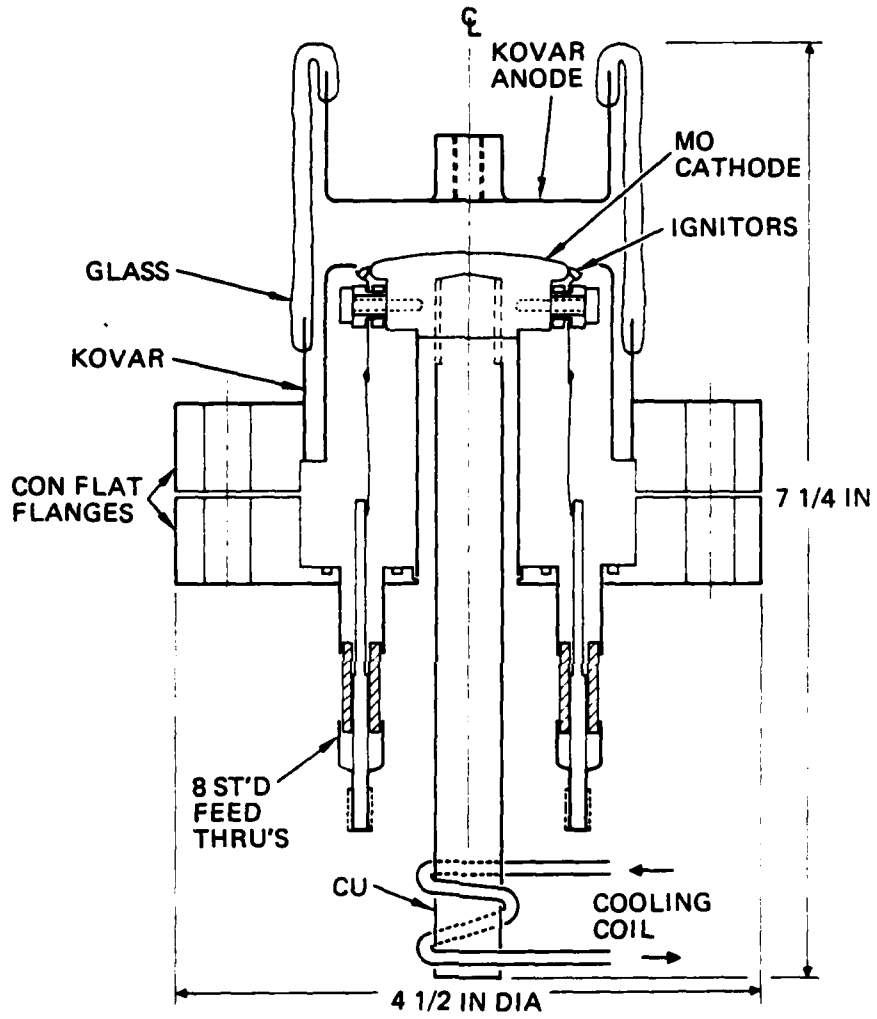


Figure 3. Cross-sectional view of OII-3.

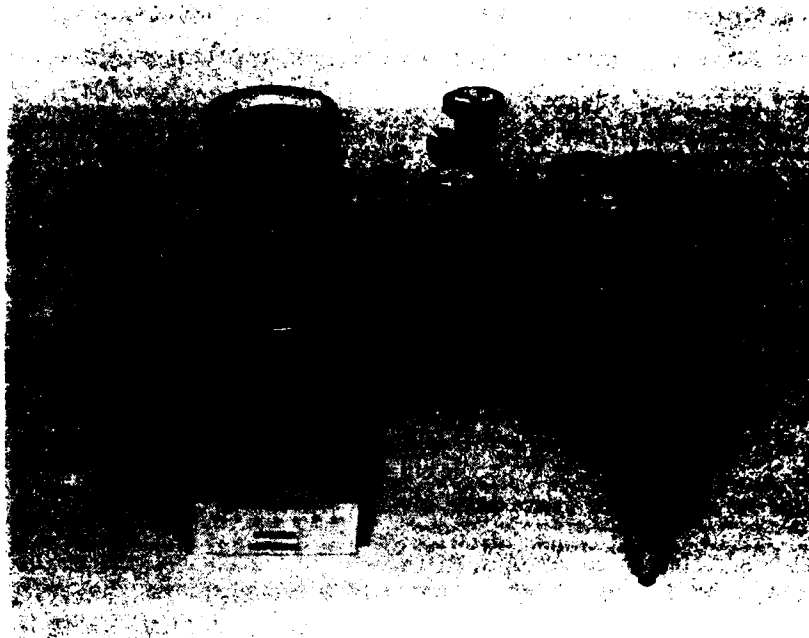


Figure 4. OII-3 completed assembly showing mercury-fill and pump-out plumbing.

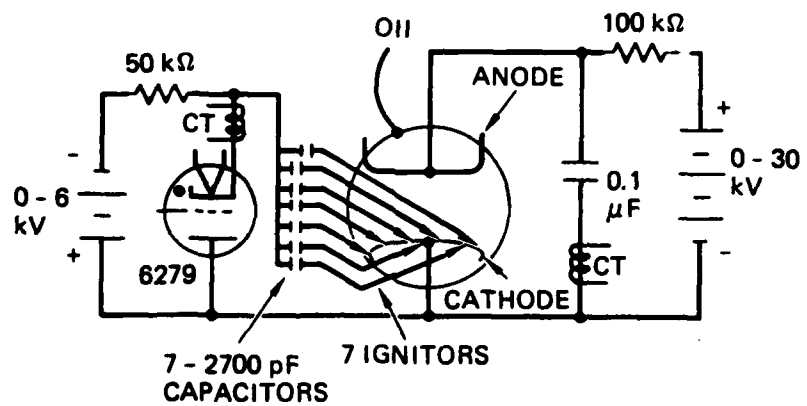


Figure 5. Test circuit for OIIs.

for the anode power supply is 0.2 A. The current in the anode circuit rings, and this results in a net average anode current an order of magnitude higher than the power supply current. The test system instrumentation includes an image converter camera, current transformers, high-voltage probes, and temperature and pressure sensors.

2. LOW POWER TEST RESULTS USING A CONVENTIONAL IGNITOR SYSTEM

The jitter behavior of the OII was examined using a conventional ignitor system design (1- μ F, 25- μ H trigger circuit) and have determined that the key source of jitter is due to the negative coefficient of resistance which is characteristic of the semiconductor ignitor tip. Switching operation, even in the absence of anode voltage, heats the ignitor material until its cold resistance of $\sim 10 \Omega$ falls below 1Ω . At this point, the semiconductor begins to run-away thermally and effectively shorts out.

The heat capacity and conductivity of the ignitor are finite so that there is a normal run time during which jitter may be low before the switch begins to misfire. The actual run time is subject to several sources of variation: contact pressure, position, Hg wetting, and initial temperature. All of these affect the initial resistance and cause fluctuations in the stable run time of the switch.

Direct current measurements show that at powers of over 1 W, the ignitor resistance falls; the ignitor voltage does not rise above about 3 V in the steady state. The thermal time constants are about 15 s.

Under pulsed conditions (Fig. 6), thermal equilibrium is not reached and the voltage can rise considerably higher than for the case of dc operation. The measured ignitor voltage starts off as though it were resistive, and it remains so as long as the voltage does not exceed about 40 V.* During this period, only a small, dim source of light is observed at the ignitor tip and anode conduction does not take place. At voltages approaching 80 V, a flashover is coincident with both the formation of a cathode spot and a drop in the ignitor voltage. The flashover appears to be essential for proper anode conduction and any jitter in its formation leads directly to jitter in the anode time-delay. The proper waveform that triggers the OII into anode conduction is that of Figure 6b.

*This is only a typical value but different ignitor tips will scale in this general fashion.

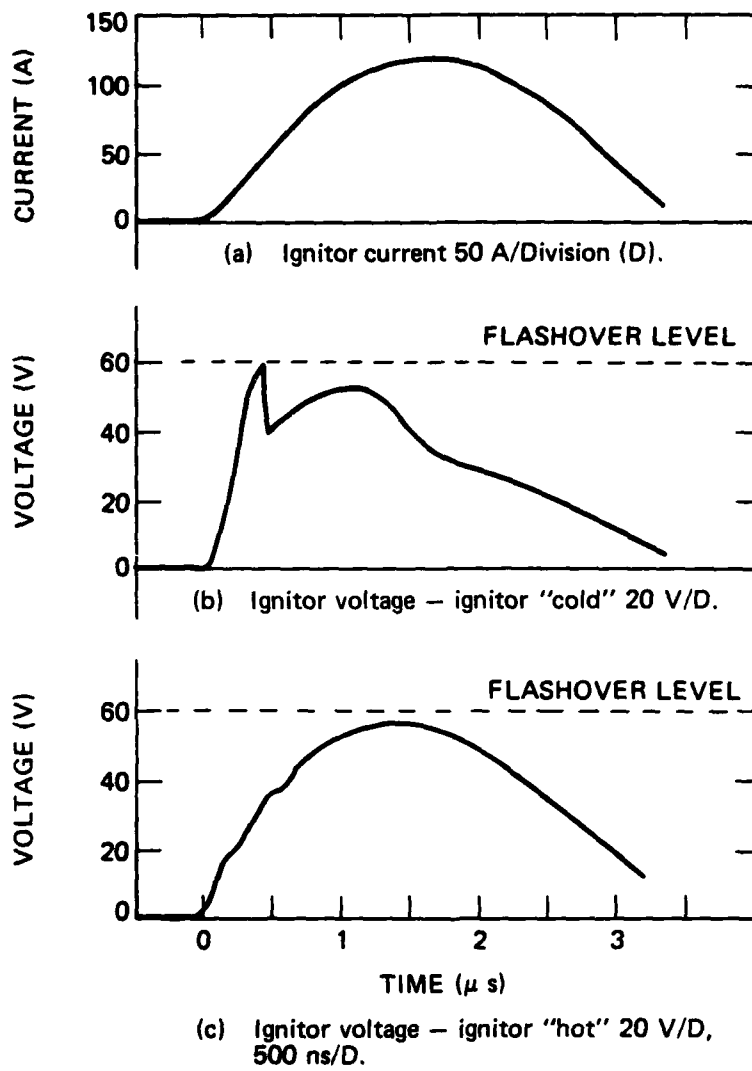


Figure 6. Pulsed ignitor characteristics.

As the ignitor heats from pulse to pulse, the peak ignitor voltage reduces until it fails to reach the flashover level (Fig. 6c) and erratic anode behavior ensues.

3. JITTER TIME CORRELATION BETWEEN PULSES

An analysis of the pulse-to-pulse correlation in anode-fall delay time has been made for a conventional ignitor system for two runs at approximately 0.5 and 1 Hz. This delay time is defined as the period from the start of the ignitor voltage waveform to the start of anode conduction. At the lower repetition rate, the jitter time σ (defined as the root-mean-square deviation) is 0.35 μ s. As the repetition rate is increased, σ increases to 0.79 μ s. Detailed analysis of the data shows that the delays are not normally distributed. A strong pulse-to-pulse correlation (i.e., memory of the previous pulse) is seen which lasts up to about 6 pulses (Fig. 7). The plot of Figure 7 shows the autocorrelation function which was made using 124 observations of delay times. Samples of 10 sequential data points were incrementally correlated with the remaining data points. Then, using the definition given by Reference 2, the next sample of 10 data points was indexed along the data list, and the correlation was repeated.

Based on these data, the purely random statistical component has a jitter of $\ll 0.3$ μ s which is superimposed upon a much larger thermal drift. The latter has a correlation time of 6 pulses or about 6 s. This is consistent with the measured ignitor temperature stabilization time of 15 s.

4. TEST RESULTS WITH A MODIFIED IGNITOR SYSTEM

The characteristics for avalanche breakdown along the surface of the ignitor are observed to be similar to other systems where a threshold voltage (V_T) is required for arcing to take place. As the trigger voltage (V) is increased beyond V_T , both the time delay (Δt) for ignitor arc development and the jitter decrease. This implies that $(V - V_T) \times (\Delta t)$ must exceed a characteristic level, which is about 5×10^{-3} V·s.

2. D.N. Menzel, Fundamental Formulas of Physics, Vol. 1 (Dover Publications, Inc., New York, NY, 1960), p. 85.

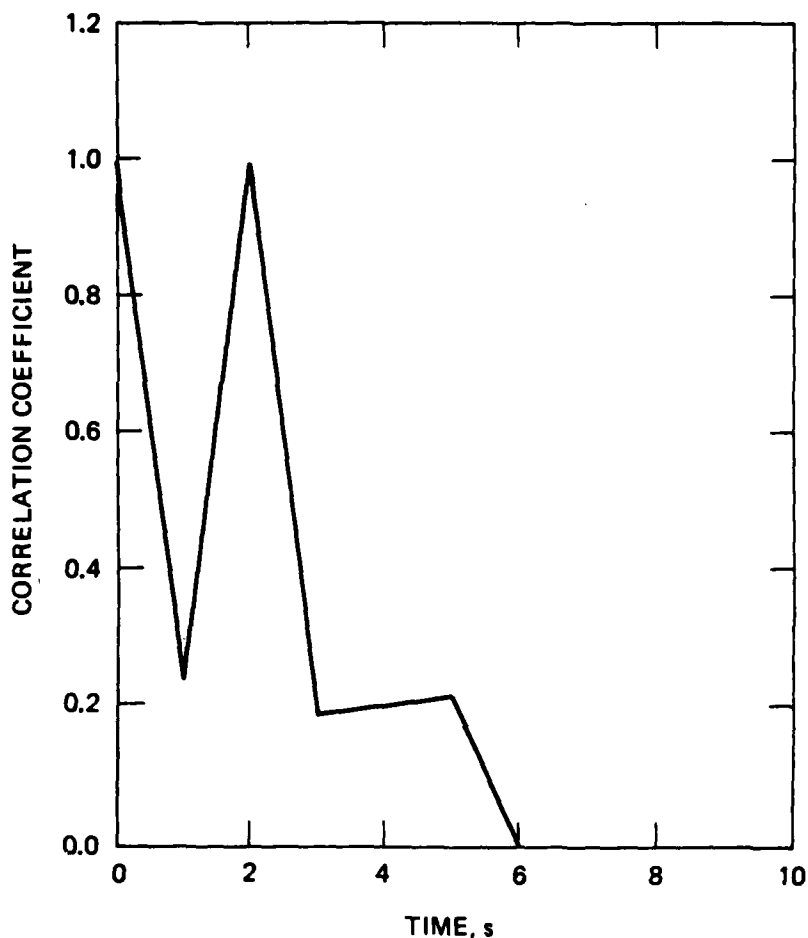


Figure 7. Interpulse correlation coefficient for jitter time for 124 observations using sample data taken at 1 and 2 Hz, using a conventional ignitor system.

Typically, the trigger circuit has a higher impedance than the ignitor, the current rise is circuit limited, and the voltage rise at the ignitor depends on the resistance (R) of the ignitor tip. Resistive heating of the ignitor depends on the temperature coefficients of the semiconductor and the design of the supporting structure. It was found empirically that during single-pulse operation the voltage first rises linearly with the current and then drops

rapidly as the resistor heats. For slow-rising pulses the resistance drops gradually early in the pulse due to Joule heating. The voltage never reaches V_T and triggering does not take place (Fig. 8c). Likewise, for very fast pulses the voltage exceeds V_T , but the resistance falls very fast and the voltage decreases below V_T before the avalanche time occurs (Fig. 8a). Proper triggering is shown in Figure 8(b) where the voltage exceeds V_T for a period long enough for an avalanche to take place, at time = t_{arc} . Measured values of the ignitor-arc delay (Δt) are shown in Figure 9 as a function of the peak ignitor voltage at 100 p/s. The trigger behavior is found to improve for smaller trigger-source capacitors which are charged to higher voltages.

5. REPETITION RATE EFFECTS (TRIGGER)

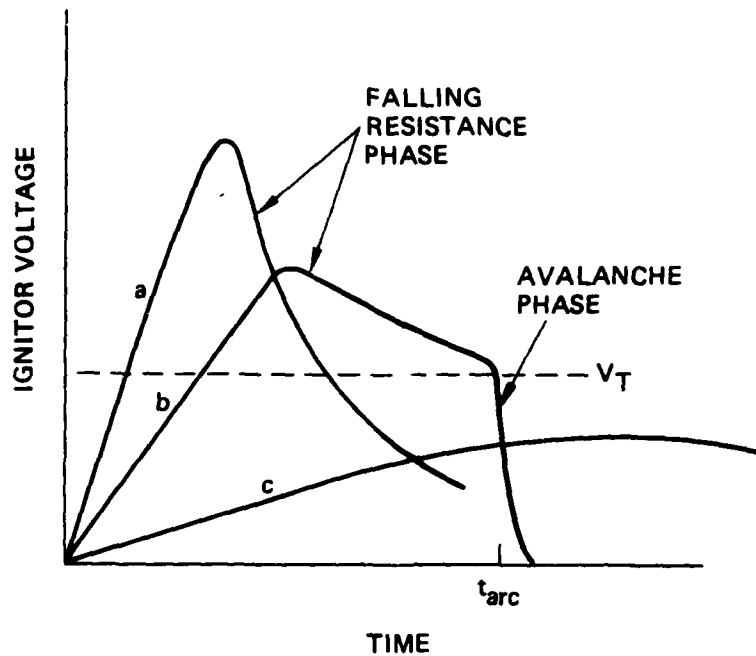
The effect of increasing the repetition rate of the trigger is to decrease the initial resistance due to heating. This reduces the stable operating range of the trigger-charging voltage and is most evident for larger capacitors. For these reasons a capacitor size of 0.0027 μF and an operating trigger voltage of about 5 kV were chosen.

Reliable steady-state operation of the ignitor was achieved at pulse-repetition rates up to 300 p/s. The steady-state trigger jitter at this frequency decreases to less than 20 ns. Start-up jitter is about 100 ns, due to thermal relaxation and is consistent with the low-repetition-rate correlation of 6 pulses.

6. ANODE CONDUCTION BEHAVIOR

The peak current capabilities of the test-model OIIs were investigated using a 4- μF capacitor in the anode circuit. Typical test results are shown in Figure 10. The anode current at 20 kA/Division (D) measures ~ 18 kA for an anode voltage of 10 kV (5 kV/D). These data are for low repetition rates (essentially single shot).

High-repetition-rate data were taken up to 300 Hz. The ratings of the laboratory dc supplies limited the high-repetition rate data to lower powers. Typical oscilloscope traces for the anode voltage and current at 100 Hz are shown in Figure 11 using a 0.1- μF trigger capacitor. Alternate scope sweeps



- (a) A fast rising current pulse produces rapid heating, the voltage pulse is high but too short to arc.
- (b) Intermediate rise time where the resistive fall is delayed and arcing has sufficient time to develop.
- (c) Slowly rising pulse where the voltage does not exceed a threshold for arc formation. Condition (b) is required for anode conduction.

Figure 8. Characteristic conditions for external avalanche breakdown along the ignitor.

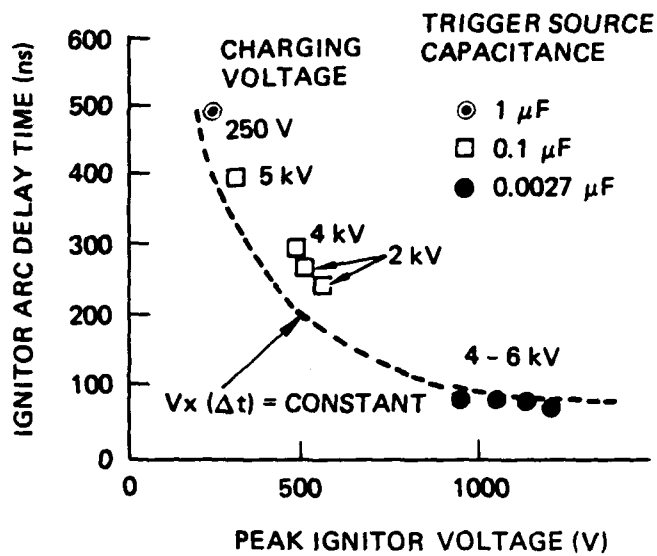


Figure 9. Ignitor arc delay time.

were used and several hundred traces are recorded, which represent operation for several seconds, near the end of a 90 s run. (The initial pulses of a run are not shown; due to circuit and thermal transients these are of greater amplitude and have more jitter.) The anode power supply is set at 10 kV; but the resistance-capacitance (R-C) charging time-constant is 10 ms, therefore the voltage reaches only about 6 kV, and the anode current is 2 kA. The jitter is about 35 ns for both the anode fall and current rise. Here, the time span at half amplitude that encompasses all the data (or ~100 pulses) is taken to be 6σ .

The anode-current-rise time is determined both by the test-circuit parameters and the OII. In Figure 12 the anode-voltage fall and current rise are shown at low repetition rate. The ignitor pulse is applied at a time, $t = 400$ ns, as can be observed on the traces by the noise burst at this time. The anode current rises exponentially from this time (400 ns) to about 1 μs . At this point (1 μs), the exponentially increasing current blends into the current

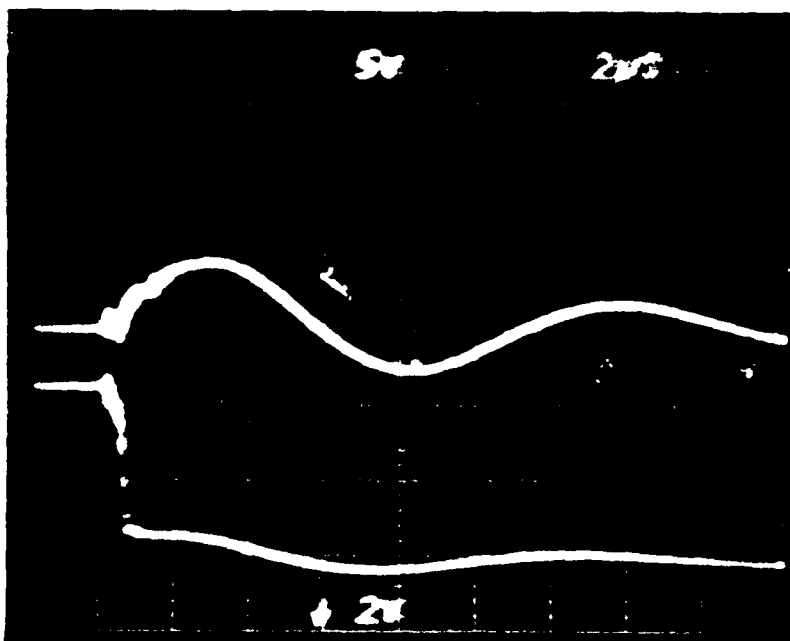


Figure 10. Operation at peak anode current of 18 kA. Anode current (top) at 20 kA/D, and anode voltage (bottom) at 5 kV/D, 2 μ S/D.

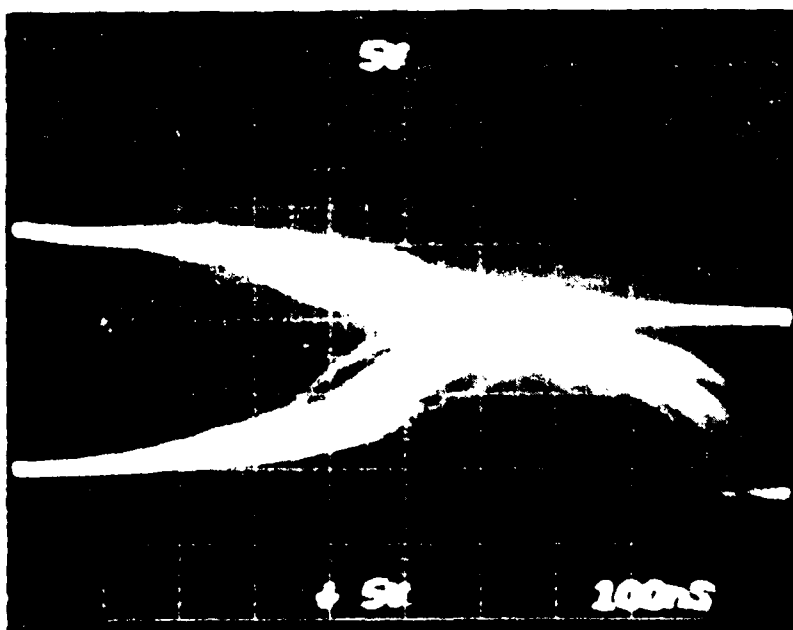


Figure 11. Operation at 100 Hz. Anode voltage (top traces) at 5 kV/D; anode current (bottom) at 1 kA/D; 100 ns/D. Showing an rms jitter of approximately 35 ns. Trigger capacitor 0.1 μ F.

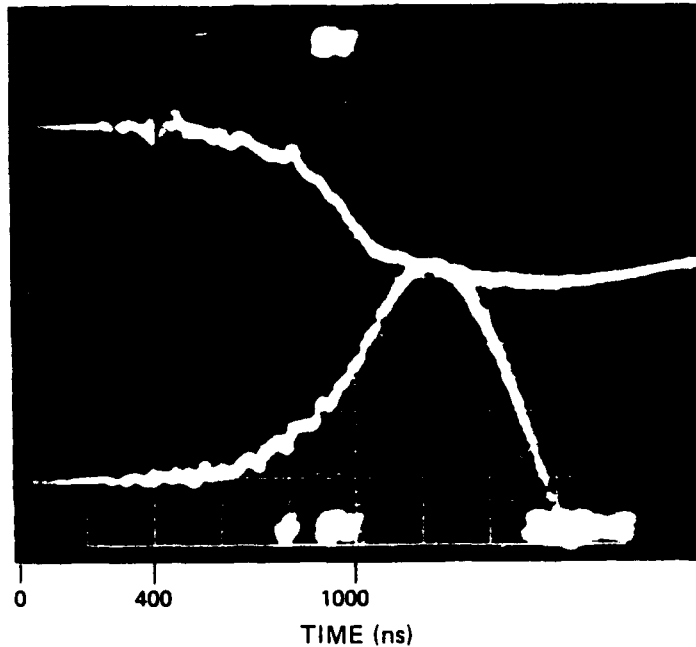


Figure 12. Anode voltage fall and current rise.
 Top - voltage at 5 kV/D.
 Bottom - current at 1 kA/D.
 200 ns/D (single pulse).

as limited by the inductance-capacitance (L-C) ringing characteristics of the test circuit. At this time, the maximum di/dt approaches $10^{10} \text{ A}\cdot\text{s}^{-1}$. The exponentially rising-current may be expressed as $I = I_0 e^{\gamma t}$ where $\gamma = 10^7 \text{ s}^{-1}$. The growth rate, γ , increases significantly with the background mercury pressure, typically produced by high-repetition-rate operation.

7. MULTIPLE IGNITORS

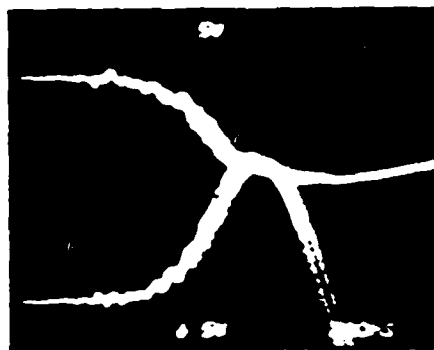
One objective of this OII development program was to study triggering characteristics as a function of the number of ignitors, the idea being to decrease jitter and increase triggering reliability with multiple ignitors. Some results are presented in Figures 13 and 14. Figure 13 shows anode voltage and current for operation with a single ignitor (a), for three ignitors (b),



(a) For one ignitor.



(b) For three ignitors.



(c) For seven ignitors.

Figure 13. Jitter as a function of the number of ignitors in use.

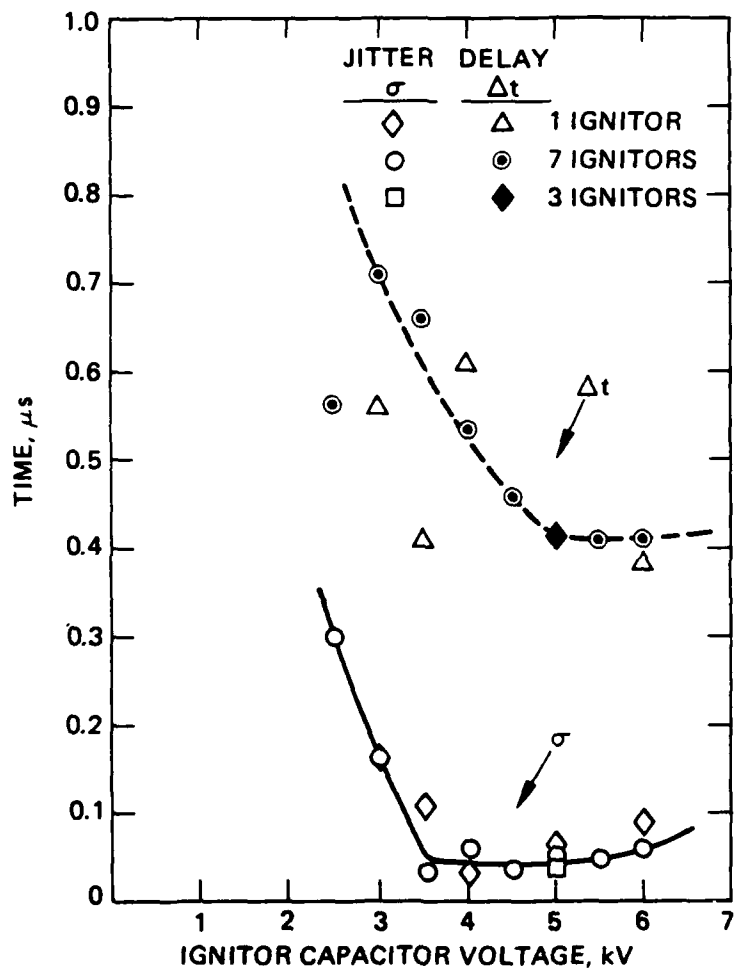


Figure 14. Low-repetition-rate jitter (σ) and delay (Δt) times as a function of ignitor capacitor voltage. Data averaged over 5 pulses. Initial anode voltage of 12 kV.

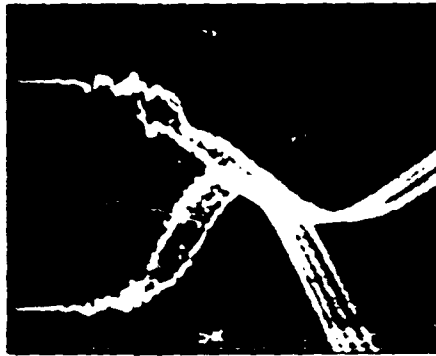
and for all seven ignitors (c). These are low repetition rate data at $V_a = 10$ kV and $I_a = 3.5$ kA. Evidently there is no significant improvement in performance by adding additional ignitors at relatively low average power. Figure 14 shows both delay time and jitter as a function of ignitor-capacitor voltage for the three cases of one ignitor (a), three ignitors (b), and all seven ignitors (c). Both delay time and jitter reach a minimum for ignitor-capacitor voltage of 4 to 5 kV and, within experimental error, the data for the multiple ignitor cases falls within the same range as that for the single ignitor case.

8. REPETITION RATE EFFECTS WITH ANODE CURRENT

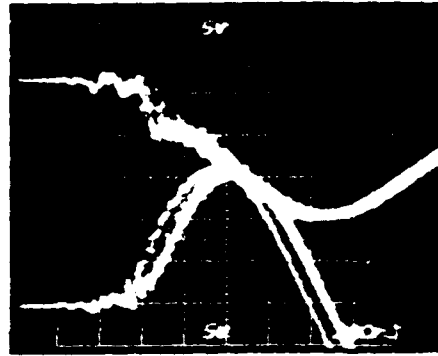
A series of measurements (Fig. 15) shows the decrease in jitter with increasing repetition rate. A trigger capacitor of 2700 pF was used. The steady-state jitter decreases appreciably from 33 ns at 1 Hz to essentially zero on this scale of 200 ns/D at 30 Hz. The jitter remains low at 60 and 100 Hz. The observation is that the temperature of the components and the Hg pressure increases and stabilizes during the runs at the higher repetition rates. This stabilization of the temperature and pressure is instrumental in the decrease of jitter. If the pressure in the OII is increased by operation at high repetition rate and followed by a reduction in the repetition rate to 1 Hz, the jitter remains low, as shown in Figure 16(a). Decreasing the pressure to its normal value of $\sim 1.5 \times 10^{-3}$ torr by pumping while hot, the jitter increases to near its previous value at 1 Hz, as shown in Figure 16(b).

9. SUMMARY OF TRIGGER IMPROVEMENTS

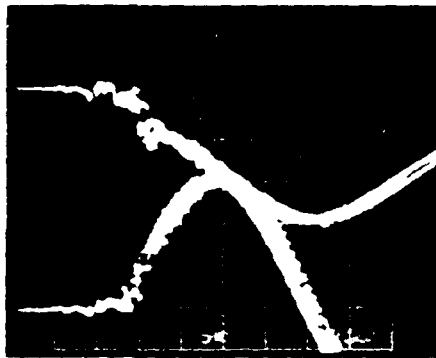
The primary trigger mechanisms leading to jitter, delay time, and switch instability at low average power have been identified in ignition type devices using mercury wetted cathodes called orientation independent ignitrons. This work has indicated the need to heat sink the ignitor electrode and limit the energy in the trigger pulse to exceptionally low levels by using higher voltages and shorter trigger pulses. These concepts were applied to the design of the ignitor and the trigger circuit and resulted in a significant improvement in switch behavior.



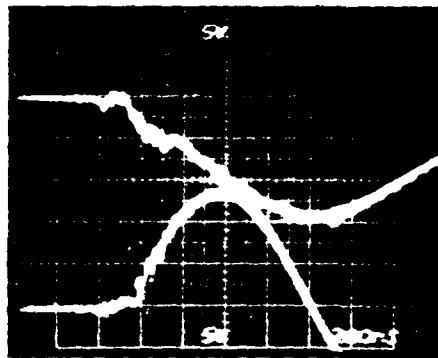
(a) At 1 Hz.



(b) At 3 Hz.



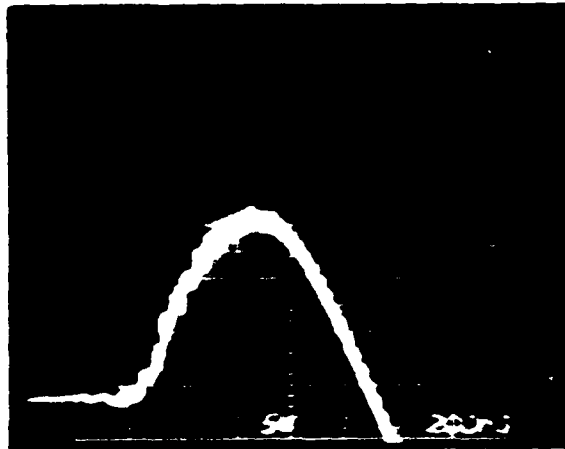
(c) At 10 Hz.



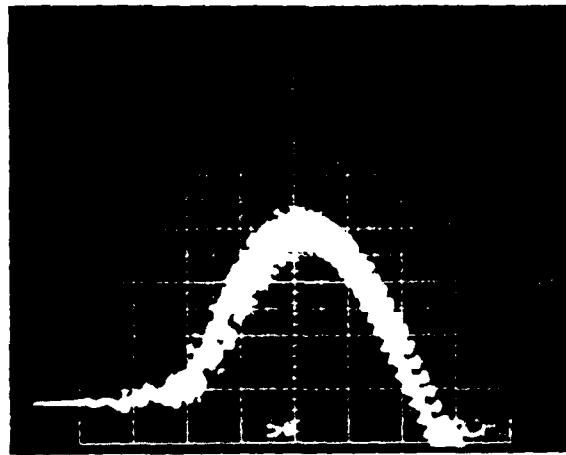
(d) At 30 Hz.

Figure 15. Jitter as a function of pulse repetition rate. Top traces, V_A at 5 kV/D. Bottom traces, I_A at 1 kA/D. 200 ns/D; 10 pulses are recorded on each figure.

Essentially steady-state operation can be maintained at frequencies beyond 300 p/s at low average power (~ 6 kW average) with jitter times much less than 20 ns. The jitter is higher during start-up transients and stabilizes as the temperature of both the ignitor and the mercury stabilize. The anode fall-time can be treated as due to an exponential growth of current. The exponential growth rate of the current is on the order of 10^7 s^{-1} at a pressure of 2×10^{-3} torr, corresponding to a starting cathode temperature of 13°C . The growth rate is automatically increased by operating the switch repetitively and increasing the mercury pressure.



(a) Pressure equals 6×10^{-3} torr.



(b) Pressure equals 1.5×10^{-3} torr.

Figure 16. Jitter as a function of OII Hg pressure. Anode current at 1 kA/D, 200 ns/D; 10 pulses are recorded on each figure.

III. HIGH AVERAGE POWER TESTS

Section II discussed low-average-power tests at Hughes Research Laboratories (HRL) which show that OIIs can be made to operate with low jitter ($\sigma \approx 30$ ns). The test limits were 30 kV, 15 kA, and 100 Hz, but these are not simultaneous data. For example, the low jitter data were obtained at low voltage and current, and the 15-kA data were obtained at low voltage. Based on these results, the OIIs were judged ready for high-average-power tests. The two test model OIIs were subsequently tested at the high-average-power facility at Kirtland Air Force Base (KAFB), New Mexico. Low-jitter data were again obtained for anode currents of 1 kA. At higher power, unstable OII operation resulted from a failure to hold voltage on recharging and failure to fire on every pulse. Sections III-1 and III-2 discuss the tests and the mechanisms responsible for the observed behavior.

1. HIGH POWER TEST RESULTS USING OII-3

OII-3 is the multiple-ignitor tube described in Section II. Two out of seven ignitor feedthrough bushings were found to be broken following shipment to the test site. These were removed and the holes were closed with epoxy. A vacuum system was arranged to pump out the tube. Cooling water for the cathode was provided using an ice bucket and pump. Typical initial test results using the high-average-power facility at KAFB are shown in Figures 17 and 18. These oscillograms show pulses accumulated on a storage oscilloscope during a 90-s run at 100 Hz. Shown in Figure 17 is the 1-kA, 28- μ s anode-current pulse. In Figure 18 the time base has been expanded to 200 ns/D, and the current rise shows low jitter (full width of 180 ns or rms deviation of $\sigma = 30$ ns).

During the early testing the tube showed a gradual improvement in behavior with current conditioning, presumably due to clean-up of contaminants. But, then as the anode voltage and current were increased, the jitter first increased by approximately an order of magnitude and then the OII failed to recover properly, as shown in Figure 19. In this figure, the anode voltage is shown at 5 kV/D and 1 ms/D. Although the OII recovered properly on most

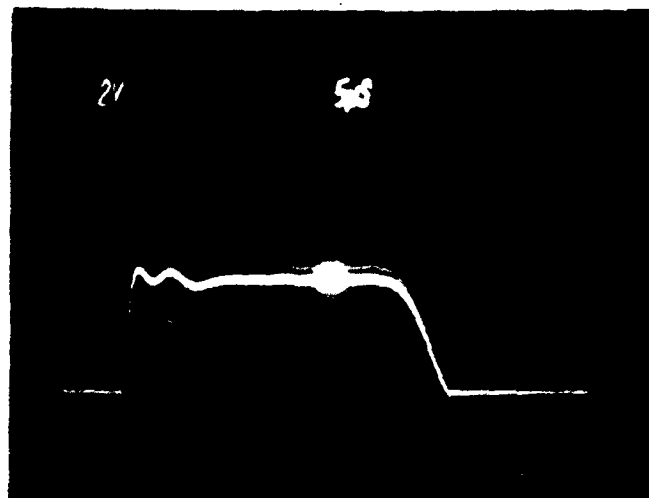


Figure 17. Anode current pulse, 1 kA x 28 ns, 400 A/D, 5 ns/D.

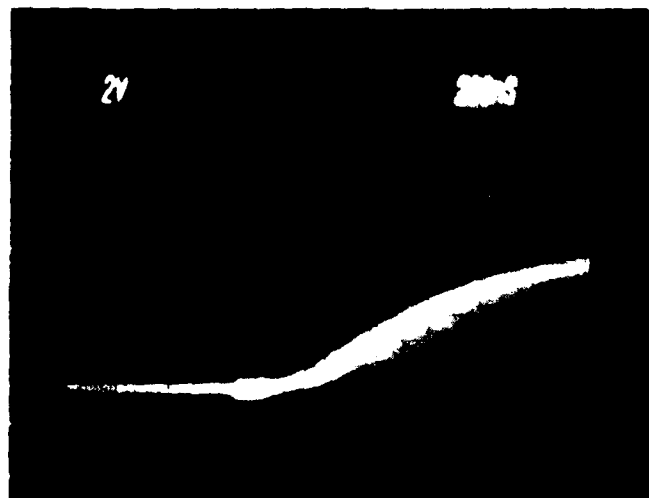


Figure 18. Anode current rise showing jitter at 100 Hz for a 90 s run period, 400 A/D, 200 ns/D, $\sigma \cong 30$ ns.

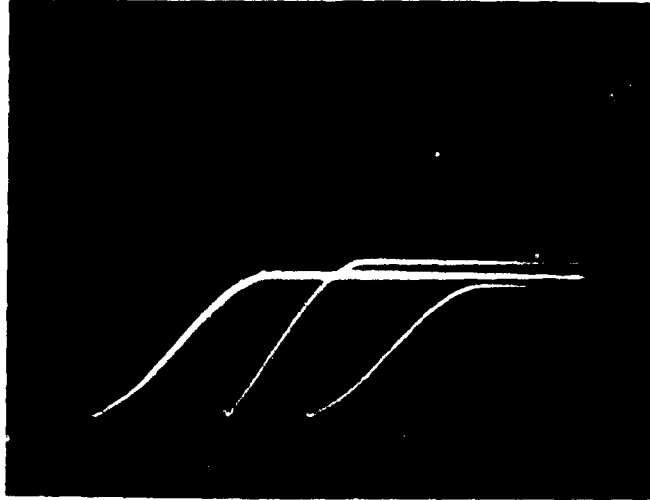


Figure 19. Anode recovery voltage at 5 kV/D, 1 ms/D.

pulses, it would on occasion conduct again without a trigger; e.g., at about 2 and 4 ms after the initial pulse, as shown in the figure. With conditioning the unstable operation initially improved. Eventually, further improvements were not obtained and failures to fire were observed.

The ignitor current-pulse was recorded to track down the possible source of both the large jitter and missing anode pulses. As shown in Figure 20, the (full width) jitter in the igniter current pulse is about 80 ns, which accounts for a sizeable fraction of the 180-ns jitter in the anode pulse. This extraneous jitter was related to instrumentation problems. However, some jitter was still switch related and some anode pulses were still missing.

OII-3 had been tested at HRL over a period of about one month and some sputtering was evidenced by a slight deposit on the glass insulator. On testing at KAFB, the sputtering was so intense that the glass envelope was completely opaque after about 1.5 days of testing. The tube behavior began to significantly degrade during that time, indicating irreversible damage.

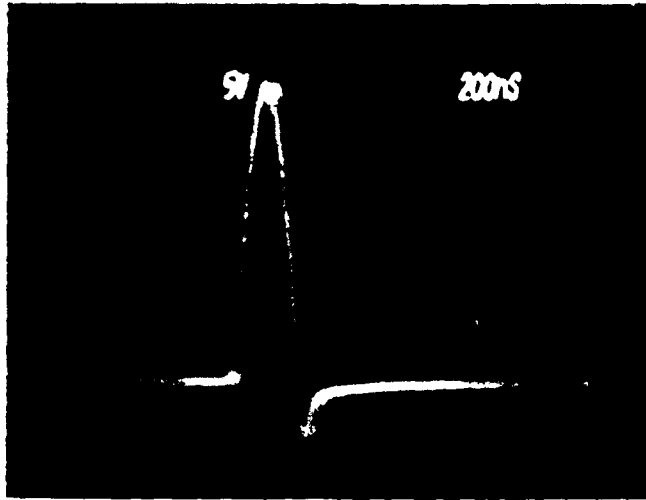


Figure 20. Igniter current pulse at 100 A/D, 200 ns/D showing residual trigger source generated jitter.

2. HIGH POWER TESTS OF OII-2

Next, the single-igniter tube, OII-2, was evaluated. The test results are summarized by referring to Figures 21, 22, and 23. In Figure 21, the anode current was found to alternate between two types of operation, a single forward pulse, and a ringing pulse. The conduction in the reverse direction is due to circuit impedance mismatch.

Figure 22 shows the anode recovery characteristics of OII-2. The switch continues to conduct for 1 msec or more on some pulses, indicating an outgassing problem. Operation was attempted at a 30-Hz rate, but before the end of a 90-s run period the tube began to fail to fire, as shown by the base line on the current pulses of Figure 23. The failures to fire were similar to those in OII-3 and the experiments were terminated.

3. ANALYSIS OF THE CATHODE SURFACE

The OIIs were dismantled for analysis. The cathode of OII-3 is shown in Figure 24. The lead to igniter No. 2 was found to be open; igniter insulators Nos. 6 and 7 were broken in shipment to KAFB, hence they were inoperable.

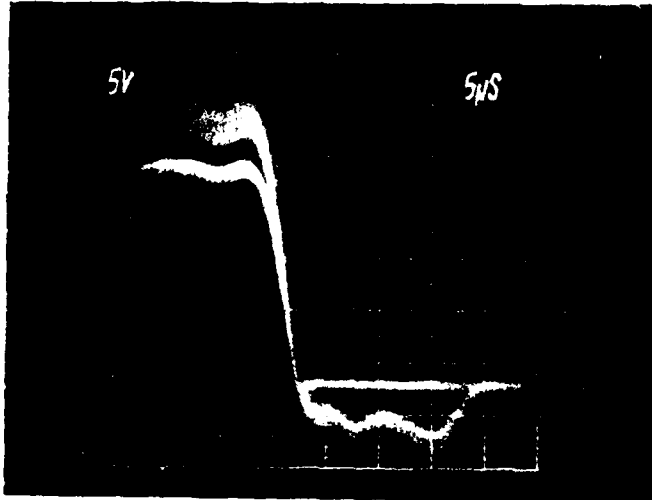


Figure 21. Anode current pulse showing reverse conduction,
1 kA/D, 5 μ s/D.

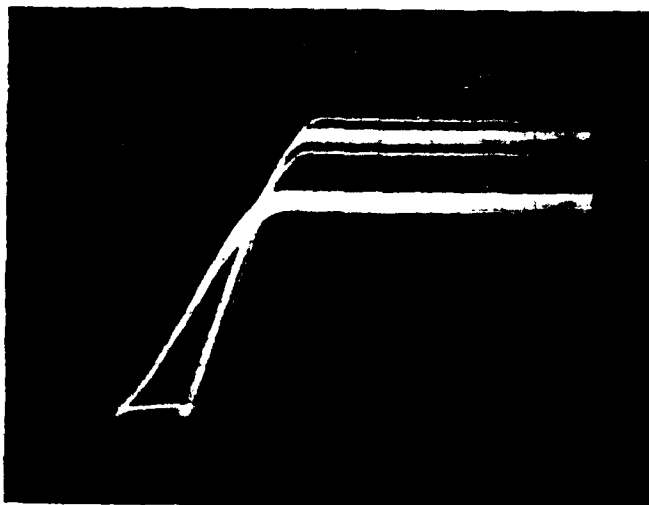


Figure 22. Anode recovery voltage for OII Mod 2, 5 kV/D,
1 ms/D.

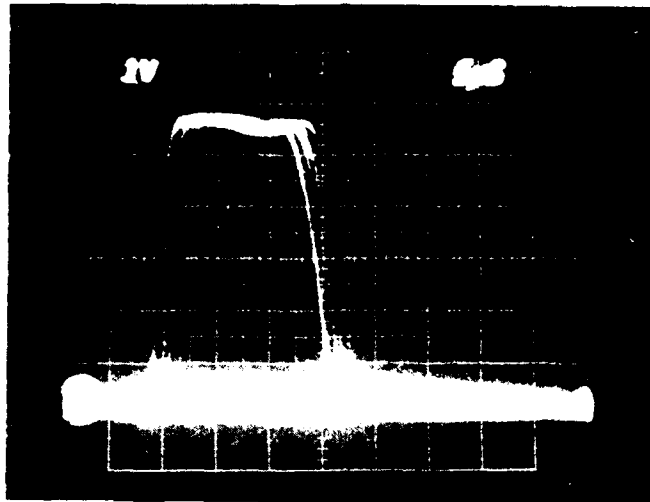


Figure 23. Anode current pulse showing missing pulses, 200 A/D, 5 μ s/D.



Figure 24. Cathode for OII - Mod 3, showing Hg depleted area (light region) and contaminated Hg layer (dark region).

Igniter No. 8 was not installed initially. The light (or active) region of the cathode is relatively Hg-free. The dark areas adjacent to the inoperative igniters Nos. 2, 6, and 7 were heavily coated with contaminated Hg. The cathode surface was studied with Auger electron spectroscopy; the dark area is apparently carbon coated in addition to being Hg coated. This carbon appears to inhibit the necessary diffusion of the Hg over the cathode surface to the regions near the active igniters.

4. DISCUSSION OF RESULTS

A 200-atom layer thickness of Hg is needed per pulse on the basis of only one electron emitted for each Hg ion evaporated. However, some estimates for the electron-to-ion ratio are as high as 50. It appears practical to deposit a sufficiently thick layer of Hg onto the cathode to supply Hg for the desired 9000 pulses. For a cathode held at 0°C, the recondensation rate of Hg onto the cathode is sufficient to pump out the Hg used during the pulse in a small fraction of the interpulse period. Therefore, it should be possible to obtain the desired voltage recovery characteristics as long as the cathode temperature is maintained. Our previous thermodynamic measurements at ERADCOM (Ref. 1) showed the cathode temperature to be normally limited to less than 60°C. Mercury starvation at the cathode could increase the heat loading beyond the safe limits, causing Paschen breakdown.

The questions arise as to why the Hg was carbon-coated and why breakdown occurs just after a pulse. Vacuum problems were experienced with both of these tubes - one was opened to air by the breakage of the ignitor insulators, while the other was opened to air by an arc at the high-voltage anode bushing. These tubes had been opened to air previously and reevaluated without deterioration of operating characteristics at low average power. High powers may increase the outgassing rate of hydrocarbons used to repair the damaged components, particularly if current reversal produces arc spots on the anode structure. Voltage breakdown just after the pulse may be related to both the pressure increase during the pulse (cracked hydrocarbons would not recondense rapidly) and the relatively large gap between the Paschen breakdown shield and the ignitor supports. Possibly, Paschen breakdown occurs from the anode, through this gap, to a region behind the cathode - a long path for a large pressure distance (P-d) product.

5. SUMMARY OF HIGH AVERAGE POWER TEST RESULTS

Switch jitter and tube failure-to-fire at high repetition rates were originally identified as due to the ignitor-trigger-system design. These trigger problems have been corrected during the present program. Additional sources of switch instability have now been identified which only occur at high average power. These are mercury starvation due to excessive heating of the cathode, lack of migration of mercury due to contamination, and overpressurization due to contamination. The cathode region reached by a single ignitor appears to be a circle about 1 cm in radius, indicating that multiple ignitors may be necessary for high average power operation if the necessary Hg recondensation rate cannot be obtained.

IV. DESIGN CONSIDERATIONS FOR A HIGH AVERAGE POWER OII

To capitalize on the increased understanding of OII operation resulting from the present program and take full advantage of the OII switch for potential military application, an OII design such as the one shown in Figure 2 should be developed which uses the multiple-ignitor design, eliminates the vacuum-leak problems, and maintains clean, uncontaminated Hg. The ignitor-shield gap should be closed up to improve the voltage-breakdown behavior. An increased Hg fill should be used and the cathode should be chilled to a lower temperature (near 0°C) for the purposes of providing sufficient Hg to solve the missing pulse problem and to help with the voltage-breakdown problem. The anode should be made of molybdenum to increase the chopping level for inverse currents and to decrease the back sputtering during current reversal. The insulators should be moved away from the arc to protect them. Under high current operating conditions, the power loading of the present cathode may reach 200 W. In a run time of only 15 s the cathode temperature may rise beyond 38°C and the mercury vapor pressure will exceed the Paschen breakdown limit. Therefore, the heat-sinking capability of the cathode structure should be increased by an order of magnitude by adding additional cathode material and copper to the heat-conductor assembly. A mass of 1 kg at the anode and at the cathode should significantly increase the stable run time of the OII to over 90 s. The OII design shown in Figure 2 includes these improvements.